

# Suspended sediment concentration and sediment transport measurements with a new two components ultrasonic profiler

Helder Guta<sup>1</sup>, Marie Burckbuchler<sup>2,\*</sup>, Stéphane Fischer<sup>2</sup>, Damien Dufour<sup>2</sup>

<sup>1</sup> Laboratory of Geophysical and Industrial Flows, Grenoble, France

<sup>2</sup> UBERTONE, Strasbourg, France

\*corresponding author: marie.burckbuchler@ubertone.fr

---

**Abstract** In order to improve understanding of the physical processes involved in sediment transport, and thus improve the capability to model such transport phenomenon, the need of high resolution measurements is evident. The results of high temporal and spatial resolution measurements of concentration and sediment flux with a new acoustic device, the UB-Lab 2C, are displayed in the present paper. This commercial ADVP was developed by the company and its conformity with another well-established acoustic system (the ACVP) and with results from previous studies performed in similar flows conditions supports its good performance for sediment flux profiling. Additionally, the shapes of mean profiles depict the well-known characteristics described in literature, namely the Rouse description of the concentration profile. Streamwise velocity, shear stress and concentration profiles, allowed the estimation of a ratio between momentum and particle diffusivities. At a given vertical range this ratio becomes nearly constant. This value corresponds to the Schmidt number, crucial in sediment flux modeling. Besides the good agreement in the estimation of the referred parameter by the two acoustic systems, it was shown that turbulence effects on settling velocity are determinant in the estimation of the Schmidt number.

**Keywords:** sediment transport, SSC, turbulence

---

## 1 Introduction

Sediment transport prediction or modelling in intense flow regimes is of great importance to a wide range of problematics (eg. river morphology, coastal bathymetry, evolution of shorelines and river banks, risks of scouring of bridges, siltation of reservoir upstream of a dam wall...). Sediment transport occurs indeed during extreme events such as floods in rivers, or storms in coastal areas, and impacts the long-term morphological evolution. During events of extreme intensity, the bedload moves as a sheet-flow, a regime characterized by the occurrence of a dense layer of particles over the sediment bed. Under such conditions, both the granular interactions and turbulent processes are the key mechanisms in the momentum diffusion driving the transport.

The prediction of sediment flux in such conditions relies on the estimation of velocity (law of the wall) and concentration (Rouse formulation) profiles. Although the Rouse profile is a physically based model, it is often required to tune a parameter that describes the ratio between the momentum and particle diffusivities, called the Schmidt number. One challenge lies in the estimation of concentration diffusivity  $\epsilon_p = w_s \phi (d\phi/dz)$ , which was found to be greater than momentum diffusivity  $\epsilon_m = \tau Q (du/dz)$  (eddy viscosity) by several researchers ([12] based on the results of [2][8][9]) and was found to be lower than eddy viscosity by [1], among others. This has an important impact on prediction of concentration profiles, but most importantly it implies different physical interpretations regarding the particle diffusion process taking place in sediment-laden flows.

In order to improve understanding of the physical processes involved in sediment transport, and thus improve the capability to model such transport phenomenon, the need of high resolution measurements is evident. However, the ability to profile within the bottom boundary layer is limited to a few measurement technologies. In the past years, an Acoustic Concentration and Velocity Profiler (ACVP) was developed at the LEGI (Laboratoire des Écoulements Géophysiques et Industriels, Grenoble, France), and revealed new insights concerning the hydrodynamic processes in the near-wall region. A prototype, called UB-MES, of a commercial version of the ACVP, named UB-Lab 2C, was developed by the French company UBERTONE. Data set of co-located 2C velocity and sediment concentration time-resolved were measured under steady

uniform turbulent rough clear water and sheet-flow, performed with the ACVP developed by LEGI and the UB-MES. In the present paper, we focus on the sediment concentration measurements performed with both devices and the same transducer. In part 2, the experimental set-up and measurements methodology are presented. The results in terms of mean profiles of velocity, concentration and sediment flux are presented in section 3. In the same section, the Schmidt number and the potential influence of turbulence in settling velocity is discussed, and the main conclusions of the paper are summarized in section 4.

## 2 Methodology

### 2.1 Experimental setup and hardware

The experiments were carried out at the LEGI, using a 10 m long tilting flume, with 0.35 m width. Different slopes were set for clear water experiments and for sheet-flow experiments. For sheet flow experiments, the (rectangular) sediment pit, located at 5 m from the beginning of the channel is 3 x 0.11 m<sup>2</sup>, is initially filled with low density ( $\rho=1192$  kg/m<sup>3</sup>) non-spherical plastic sediments (Poly-Methyl MethAcrylate) of median diameter  $d_p=3$  mm and the packed volumetric concentration is 0.55. The settling velocity  $w_s$  of the particles is 5.6 cm/s. The fixed bed is covered by glued particles, with the same properties as the sediments filled in the channel. For the clear water measurements, the fixed bed is placed in the sediment pit. For both conditions (clear water and sheet flow), a sluice gate at the downstream end and a by-pass at the upstream end allow to regulate the flow discharge as shown in figure 1.

One of the major differences between the two systems is that the UB-MES is portable, easily displaceable, as result is limited in terms of continuous data flow load, while the ACVP is not portable, however, no limitations are encountered in terms of data flow load. For both acoustic systems, the carrier frequency was set to 1 MHz, with a pulse duration of 2  $\mu$ s allowing a vertical spatial resolution of 1.5 mm. The obtained time resolutions were 19 Hz for velocity and 4.8 Hz for concentration, for sheet-flow measurements.

### 2.2 Experimental protocol and flow properties

The sheet-flow experimental protocol from [8] was applied. The experiments are performed with no recirculation of the sediments. In such conditions, after a short period at the beginning of the experiment, the sediments placed in the pit are eroded (see figure 1). Each experiment lasted less than two minutes. Thus for proper statistical convergence of the flow quantities, the experimental runs were repeated several times (N=4 with ACVP and N=5 for UB-MES). Following this protocol, there is an initial transient phase, in which the bed erosion rate reaches its peak value, followed by a quasi-uniform phase of the flow, with a fairly steady bed erosion rate, which lasts about 30 s, and a final phase of high instability, as the bed is significantly disturbed due to erosion. Only the measurements in the quasi-uniform phase are considered for the hydrodynamic analysis.

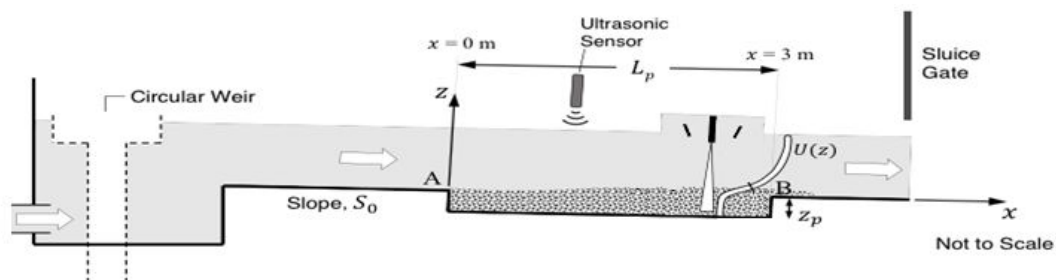


Fig. 1 Sketch of experimental set up

For clear water experiments, no particular protocol was implemented since the sediment pit was covered by fixed rough bed plates. It was only necessary to approach the uniform flow conditions for which the mean flow and turbulence properties are well known and described in the literature [7].

For both clear water and sheet-flow conditions, the flow was highly turbulent, hydraulically rough and subcritical (Table 1), as indicated by the high Reynolds number ( $Re \gg 2000$ ), the high bed roughness

Reynolds number ( $Re^* \gg 70$ ) and the low Froude number ( $Fr < 1$ ).

Table 1. Sediment and flow properties in Clear water (CW) and Sheet-flow (SF)

	$S_0$ (%)	$d_p$ (mm)	N (-)	$w_s$ (cm/s)	$u_*$ (cm/s)	$\rho_p$ (kg/m <sup>3</sup> )	$H_f$ (m)	$Q$ (m <sup>3</sup> /s)	$U$ (m/s)	Re (-)	Re* (-)	Fr (-)
CW <sub>(ACVP &amp; UB-MES)</sub>	0.375	-	-	-	5.7	-	0.12	28.9	0.69	$8 \cdot 10^4$	428	0.6
SF <sub>(ACVP)</sub>	0.5	3.0	4	5.6	4.3	1192	0.135	28.8	0.59	$8 \cdot 10^4$	304	0.5
SF <sub>(UB-MES)</sub>	0.5	3.0	5	5.6	4.1	1192	0.145	28.8	0.55	$8 \cdot 10^4$	322	0.5

$S_0$ : Slope of the channel;  $U$ : bulk mean velocity;  $H_f$ : water depth;  $\nu$ : kinematic viscosity of water;  $u_*$ : friction velocity;  $ks$ : equivalent roughness ( $ks=2.5 d_p$ ) and  $g$  is the gravitational acceleration.

## 2.3 Velocity and Concentration measurements with ACVP and UB-MES

### 2.3.1 Velocity measurement

The velocity profiling principle in both acoustic systems relies on the measurements of Doppler frequencies. By employing one emitter and two receivers, two Doppler frequencies along the common emitter axis can be measured. From these quasi-instantaneous Doppler frequencies, one streamwise  $u$  and one vertical velocity  $w$  are retrieved.

### 2.3.2 Concentration measurement with ACVP

The output of the mean squared voltage signal of the ACVP is [5]:

$$I_{mo} = A_{mo} A_s C e^{-4 \int_0^r -4\zeta_s C dr} \quad (1)$$

where,

$$A_{mo} = R_0^2 \frac{\pi c}{4} e^{-4\alpha_w r} \quad (2)$$

$$A_s = \frac{3}{4\rho_p} \frac{\{a^2 f^2(\theta=\pi, ka)\}}{\{a^3\}} \quad (3)$$

$$\zeta_s = \frac{3}{4\rho_p} \frac{\{a^2 \chi(\theta, ka)\}}{\{a^3\}} \quad (4)$$

The term  $A_{mo}$  includes the system dependent parameters and the water absorption term along the profile.  $R_0$  is a system constant valid for the transducer sensitivity and the transfer function of the hardware unit,  $\tau$  is the duration of the pulse,  $r$  is the range of the transducer,  $c$  is the speed of sound in water and  $\alpha_w$  is the water attenuation constant for pressure. The term  $A_s$  is the particle backscattering term, i.e. for  $\theta=\pi$ . The  $\zeta_s$  is the attenuation coefficient. The term  $ka$  product of the wave number,  $k$ , and particle radius,  $a$ . The functions  $f(\theta=\pi, ka)$  and  $\chi$  are the fundamental backscattering form function and the normalized total scattering cross section, respectively. The former describes the backscattering characteristics of the elementary particles and the latter describes the scattering attenuation characteristics of the suspension. The curly brackets denote averaging weighted by the size distribution of the particle suspension  $n(a)$ , such that the mass concentration can be written as:

$$C = N_p \rho_p \frac{4}{3} \pi \int_0^\infty a^3 n(a) da \quad (5)$$

where  $N_p$  is the numerical density number(number/m<sup>3</sup>) of mean radius  $as = \{a\} = \int_0^\infty an(a) da$ .

Thus, knowing  $A_{mo}$ ,  $f$ ,  $\chi$ ,  $a_s$  and  $n(a)$  a priori, the volumetric concentration profile was obtained by inverting equation (1), following the same inversion method as in [4].

### 2.3.3 Concentration measuring principle with UB-MES

Acoustic intensities backscattered by air bubbles are subtracted from the total intensities, in order to retrieve solely the particle echo intensities. The echo from air bubbles is estimated in CW flows. It was observed that the intensity profiles from ACVP and UB-MES in CW display a proportional relationship. Figure 2 shows the profiles of intensities of UB-MES (blue) and ACVP (red) after applying the observed proportionality constant. It is seen that intensity profiles of both acoustic systems display the same behavior, both qualitatively and quantitatively. As result, it was possible to perform the same inversion procedure of ACVP to the UB-MES, in order to retrieve the concentration profiles, in sheet-flow.

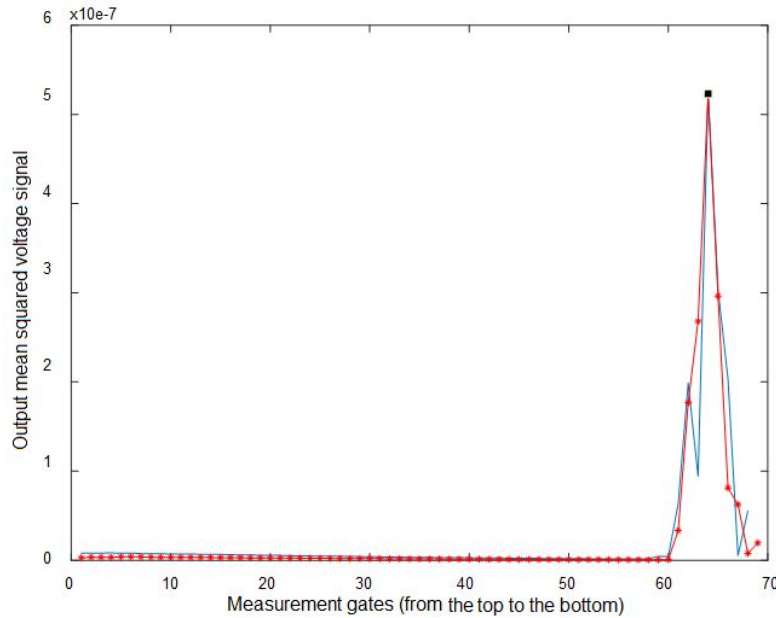


Fig. 2 Comparisons between echo intensities from UB-MES (blue) and ACVP (red,\*) in CW applying the determined proportionality constant

Note that the echo intensity profiles display a sudden increase. This corresponds to the bed position (solid boundary), where the backscattered echo is significantly higher when compared with the air bubbles. This principle serves as the basis for the detection of the bed position instantaneously, under sheet-flows.

## 3 Results

### 3.1 Mean Profiles

By comparing mean velocity profiles, concentration and sediment flux measured by the ACVP and by UB-MES, the sediment flux profiling capability of UB-MES is analyzed in this section. The friction velocity  $u^*$  estimated from the extrapolated Reynolds shear stress, was about 4.1 cm/s for UB-MES and 4.3 cm/s for ACVP. The corresponding Shields number was about  $\theta=0.3$  for both systems, and it shows also a good agreement with respect to [4], in which  $u^*=4.1$  cm/s. The suspension number,  $w_s/u^*=1.4$  and  $w_s/u^*=1.3$  for UB-MES and ACVP respectively.

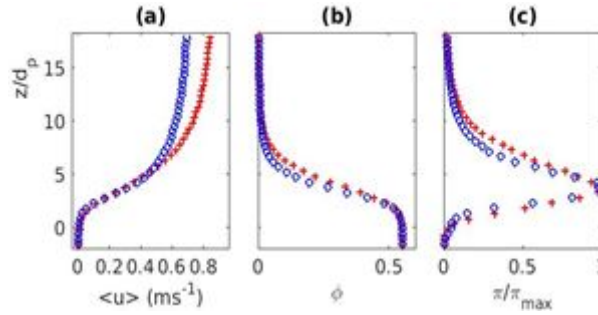


Fig. 3 Mean streamwise velocity (a), concentration (b) and normalized sediment flux (c) depending on the normalized depth, for ACVP (+) and UB-MES (o)

Figure 3a displays the mean streamwise velocity profiles for ACVP (+) and UB-MES (o). The relative difference between UB-MES and ACVP increased with elevation up to 14% at the top of the profiles. Such difference is attributed to different flow conditions, despite the same flow regime, as indicated by the same order of magnitude of the flow parameters.

Figure 3b shows that concentration decreased with increasing  $z$ , from its maximum value 0.55, with distinct trends along the flow depth. It decreased linearly for  $2 < z/dp < 4$  and then it decreased exponentially with  $z$ , as the well-known Rouse [10] profile. Rouse's equation allows the estimation of concentration  $C$  at any distance  $z$  from the bed:

$$C = Cr \left( \frac{H_f - z}{z} \frac{H_r}{H_f - H_r} \right)^{\frac{w_s}{\sigma \kappa u_*}} \quad (6)$$

where  $Cr$  is a reference concentration at a reference level  $H_r$ ,  $H_f$  is the water flow depth,  $\kappa$  is the Von Karman parameter and  $u^*$  is the friction velocity,  $w_s$  is the settling velocity and  $\sigma$  is the Schmidt number. This equation provides good results if all parameters are well estimated. However, in many cases the uncertainties on these parameter are important. In this context, the Schmidt number will be discussed with more detail in the next subsection.

The vertical distribution of the sediment flux normalized by its maximum value is presented in Figure 3c. The ACVP displays slightly wider flux profiles than the UB-MES. The mean sediment flux  $\pi$  (per meter width, over the quasi-steady interval) estimated with UB-MES and ACVP are respectively 7.5 and 9.3 m<sup>2</sup>/s. The relative difference in mean sediment flux predicted by the UB-MES with respect to ACVP is below 20%, which strongly suggests the good capabilities of the UB-MES to measure sediment flux. The lower mean sediment flux observed in the UB-MES measurements with respect to ACVP is consistent with the observed differences in terms of velocities. This confirms that the flow was slightly more energetic during measurements with the ACVP. To compare with the measured values, the sediment flux was estimated by [6] in the adimensional form, [3] and [13] by equations 7, 8, and 9, respectively:

$$\psi = 8 (\theta - \theta_c)^{3/2} \quad (7)$$

$$\pi = 0.05 * U^2 * \frac{d}{\Delta * 9.81}^{0.5} * \theta^{1.5} \quad (8)$$

$$\pi = \frac{12.5 * \frac{\sigma \Gamma_0}{\Delta * w_s} * (u_*^2 - u_{*c}^2)}{\rho_p * 9.81} \quad (9)$$

Dimensionless form of the sediment flux per unit width can be obtained from:

$$\Psi = \frac{\pi}{\sqrt{g(s-1)^3}} \quad (10)$$

where  $\psi$  is the dimensionless sediment flux,  $\theta_c=0.05$  is the critical threshold value for initiation of particle motion,  $\Delta$  is the difference between the relative density of particle and fluid and  $s=1.192$  is the relative density of particles. The relative error from these predictions with respect to the measured values are also presented in Table 2, estimated as:

$$E (\%) = \frac{\Psi_i - \Psi_{Measured}}{\Psi_{Measured}} * 100 \quad (11)$$

where  $\psi_i$  is the dimensionless mean sediment flux estimated from the referred methods and  $\Psi_{Measured}$  corresponds to the measured mean sediment flux. In Table 2, sediment flux and its relative error are given for measurements with the ACVP, with the UB-MES, as well as the results from [4].

Table 2. Dimensionless mean sediment flux and relative error of mean sediment flux by [6], [3] and [13] with respect to the measured values

	ACVP		UB-MES		Fromant et al. (2018)	
	$\psi$	E (%)	$\psi$	E(%)	$\psi$	E(%)
Measured	4.1		3.3		3.7	
[6] - Meyer-Peter & Muller (1948)	1.0	75.8	0.9	74.7	1.0	73.2
[3] - Engelund & Hansen (1967)	0.5	87.6	0.4	88.7	0.5	87.3
[13] - Yang & Lim (2003)	1.7	58.5	1.3	66.2	1.3	66.2

Yang and Lim formula shows closer values to the measured ones, however, in general a poor agreement is observed for all the proposed methods. This is a recall regarding the inaccuracies of the sediment transport models, which is in the core of the need of high resolution measurements.

### 3.2 Momentum and particle diffusivities

The Schmidt number  $\sigma_s$  relates the momentum ( $\epsilon_m$ ) and particle diffusivity ( $\epsilon_p$ ):

$$\sigma = \frac{\epsilon_m}{\epsilon_p} \quad (12)$$

Rouse [10] assumed  $\sigma_s=1$  initially, however, further analysis concluded that it may vary significantly from 1. The momentum diffusivity, with the same dimension as kinematic viscosity, can be estimated as:

$$\epsilon_m = \frac{\tau}{\rho_m \left| \frac{dw}{dz} \right|} \quad (13)$$

From the equilibrium between upward turbulent dispersion and downward sediment flux, the particle or concentration diffusivity can be defined as follows:

$$\epsilon_p = \frac{w_s \varnothing}{\left| \frac{dw}{dz} \right|} \quad (14)$$

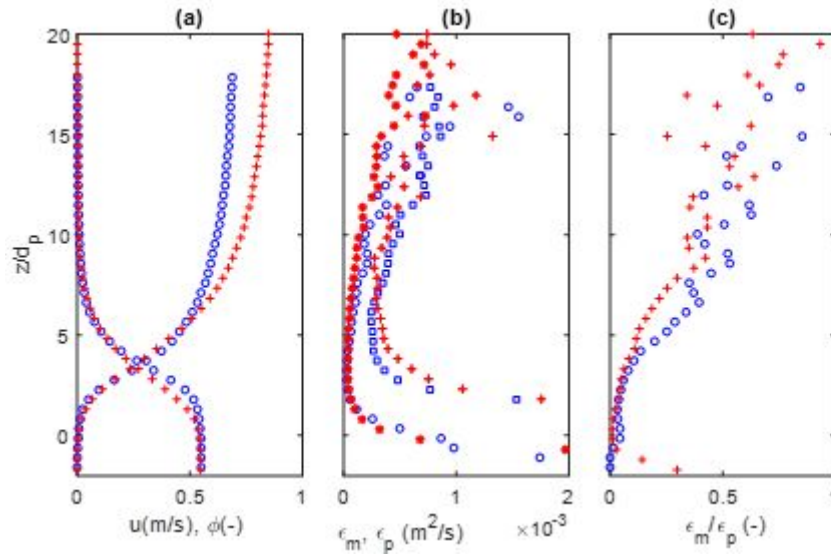


Fig. 4 Mean velocity and concentration profiles (a), momentum diffusivity (o,\*) and concentration diffusivity (,+□) (b), ratio between the momentum diffusivity and particle diffusivity (c); for UB-MES (blue ,o) and ACVP(red,+).

Momentum and concentration diffusivity profiles are shown in figure 4b. One observes that the concentration diffusivity is greater than the momentum diffusivity, however, the ratio between them becomes constant roughly in the same range where the mixing length is seen to be linear. A physical interpretation for  $\sigma_s < 1$ , proposed by [11], is the presence of centrifugal forces acting on the particles (higher density) causing particles to be thrown outside of the eddies with a consequent increase of the effective mixing length. The conclusions from [12] suggested that this is the main physical process. The Schmidt number was found to be approximately  $\sigma = 0.40$  for both systems, while [8]  $\sigma = 0.44$ .

Comparisons between upward flux  $\epsilon_p \frac{d\phi}{dz}$  and the measured vertical flux  $w'\phi'$  provides insights into the settling velocity modifications due to turbulence. Differences between them are attributed to the fact that in highly turbulent flows the settling velocity is not the same as in quiescent water condition. Although not displayed here, this analysis showed that the measured settling flux is considerably lower than  $w_s\phi$ , suggesting that there is an important reduction in the settling velocity in presence of highly turbulent flows. Taking this into account when estimating the particle diffusivity it would significantly decrease its value, and as consequence it gives  $\sigma_s > 1$ . [1] proposed that  $\sigma_s > 1$  because sediment particles cannot fully respond to the turbulent velocity fluctuations, which were assumed to be one-dimensional. In fact, a full description of the physical process governing the departure of Schmidt number from unity is not available yet [8]. Thus, by taking different types of sediments and flow regimes, the velocity and concentration measurements with these acoustic systems can provide important insights concerning the physical phenomena behind particle diffusion process in mobile-bed flows.

## Conclusions

The UB-Lab 2C capabilities of high-resolution profiling of concentration and sediment flux under sheet-flow conditions has been highlighted. The conformity of the UB-Lab 2C with another acoustic system (the ACVP) and with results from previous studies performed in similar flows conditions supports its good performance for sediment flux profiling. Additionally, the shapes of mean profiles have shown to display the well-known characteristics described in literature, namely the logarithmic behavior of the velocity profile and the Rouse description of the concentration profile. Thanks to the measurement of two components (2C) velocity and concentration profiles, the Schmidt number was estimated. It was observed a value lower than unity, indicating that particle diffusivity is greater than that of the fluid. Additionally, caution should be taken when evaluating the settling velocity in highly turbulent flows, as it may decrease significantly from the quiescent water value, thus affecting drastically the predicted particle diffusivity. The utility of further studies with different sediments and flow regimes was underlined to understand better the physical phenomena behind

particle diffusion process in mobile-bed flows.

Moreover, acoustic measurement technique allows to give information on grain size distribution by using several emission frequencies. The hardware of the UB-MES is being tested in the DEXMES facility using other emission frequencies on different suspended solids natures and concentrations in well-known laboratory conditions and comparing the results to other types of sensors (OBS, ABS, ...) to determine which possibilities this technology could offer.

### Acknowledgment

The authors are grateful for the support of the French DGA through the ANR ASTRID program.

### References

- [1] Carstens, M. R. (1952) Accelerated motion of a spherical particle. *Transactions of the American Geophysical Union*, v. 33, pp 713–721.
- [2] Coleman, N.L (1970) Flume studies of the sediment transfer coefficient. *Water Resour Res* 6(3), pp 801–809.
- [3] Engelund, F. & Hansen, E. (1967) A monograph on sediment transport in alluvial streams. *Technical Press* (Teknisk Forlag), Copenhagen.
- [4] Fromant, G., Mieras, R.S., Revil-Baudard, T., Puleo, J. A., Hurther, D. & Chauchat, J. (2018) On bed load and suspended load measurement performances in sheet-flows using acoustic and conductivity profilers. *J. Geoph Res: Earth Surface*.
- [5] Hurther D, Thorne P D, Bricault M, Lemmin U and Barnoud J M (2011) A multifrequency acoustic concentration and velocity profiler (ACVP) for boundary layer measurements of fine-scale flow and sediment transport processes, *Coastal Engineering*. 58, pp 594–605.
- [6] Meyer-Peter, E. & Muller, R. (1948) Formulas for bed-load transport. In: 2nd Meeting of the International Association of Hydraulic and Structural Research, pp 34–64.
- [7] Nezu I. and Nakagawa H (1993) *Turbulence in Open-channel Flows*. Rotterdam, Balkema.
- [8] Revil-Baudard T, Chauchat J, Hurther D. and Barraud P A (2015) Investigation of sheetflow processes based on novel acoustic high-resolution velocity and concentration measurements. *J. Fluid Mech.* 767, pp 1–30.
- [9] Revil-Baudard T, Chauchat J, Hurther D and Eiff O A (2016) Turbulence modifications induced by the bed mobility in intense sediment-laden flows; *J. Fluid Mech.*, 808, pp 469 - 484.
- [10] Rouse, H. (1937). Modern conceptions of the mechanics of turbulence. *Trans. Am. Soc. Civ. Eng.* 102, pp 463–505.
- [11] Singamsetti, S. R. (1966) Diffusion of sediment in a submerged jet. *J. Hydraulics Div.*, ASCE, Vol 92, No. HY2.
- [12] Van Rijn, L.C. (1984b) Sediment transport, part II: suspended load transport. *J Hydraul Eng* 110(11), pp 1613–1641
- [13] Yang, S.Q. & Lim S.Y. (2003) Total load transport formula for flow in alluvial channels. *J Hydraul Eng* 129(1), pp 68–72